

# **IMPROVED SEISMIC HAZARD MODEL WITH APPLICATION TO PROBABILISTIC SEISMIC DEMAND ANALYSIS**

Brendon A Bradley<sup>1\*</sup>, Rajesh P Dhakal<sup>1</sup>, Misko Cubrinovski<sup>1</sup>, John B Mander<sup>1</sup>, Greg A MacRae<sup>1</sup>,

<sup>1</sup>Department of Civil Engineering, University of Canterbury, Private Bag 4800, Christchurch 8020, New Zealand

\*Corrospoding author: Ph +64-3-366 7001 ext 7673; Fax: +64-3-364 2758;

Email: bab54@student.canterbury.ac.nz

## **ABSTRACT**

An improved seismic hazard model for use in performance-based earthquake engineering is presented. The model is an improved approximation from the so-called 'power law' model, which is linear in log-log space. The mathematics of the model and uncertainty incorporation is briefly discussed. Various means of fitting the approximation to hazard data derived from probabilistic seismic hazard analysis (PSHA) are discussed, including the limitations of the model. Based on these 'exact' hazard data for major centers in New Zealand, the parameters for the proposed model are calibrated. To illustrate the significance of the proposed model, a performance-based assessment is conducted on a typical bridge, via probabilistic seismic demand analysis (PSDA). The new hazard model is compared to the current power law relationship to illustrate its effects on the risk assessment. The propagation of epistemic uncertainty in the seismic hazard is also considered. To allow further use of the model in conceptual calculations, a semi-analytical method is proposed to calculate the demand hazard in closed-form. For the case study shown, the resulting semi-analytical closed-form solution is shown to be significantly more accurate than the analytical closed-form solution using the power law hazard model, capturing the 'exact' numerical integration solution to within 7% accuracy over the entire range of exceedance rate.

## **KEYWORDS**

performance based earthquake engineering (PBEE); probabilistic seismic demand

analysis (PSDA); seismic hazard model; demand hazard.

## INTRODUCTION

Performance-based earthquake engineering (PBEE) has emerged as a cornerstone of modern earthquake engineering as it attempts to capture the performance of structures over the full spectrum of structural behaviour, from initial elastic response through to global instability, when subjected to a range of ground-motion excitations. Seismic performance can be presented in various forms, some of the most common being: annual rate of exceeding some structural demand parameter; annual rate of exceeding some financial loss; expected annual loss (EAL); and the probability of exceeding some loss given an earthquake scenario. In order to obtain the majority of the above measures, relationships must be defined between: seismic intensity and recurrence rate; seismic intensity and structural demand; and structural demand and financial loss. The focus of this paper in particular is the relationship describing the occurrence over time of a given ground-motion intensity measure. This relation, commonly in the form of a ground-motion intensity measure and annual rate of exceedance, is typically obtained by conducting probabilistic seismic hazard analysis (PSHA) [1-3]. It is advantageous to define a relationship to represent this so-called ‘seismic hazard curve’ so that PBEE assessments can be made using analytical or numerical integration techniques, allowing for the propagation of uncertainty in the hazard model.

Sewell *et al.* [4] proposed the following power law expression for the relationship between annual rate of exceedance and ground-motion intensity:

$$v(IM) = k_0 IM^{-k} \quad (1)$$

Where  $IM$  = ground-motion intensity;  $v(IM)$  = annual rate of exceedance of a ground-motion of intensity  $IM$ ; and  $k_0$  and  $k$  are empirical constants. As seismic hazard curves are typically plotted on a log-log scale, Equation 1 is linear in log-log space. This form of

parametric equation is primarily used when combined with a similar power law relationship for seismic intensity to demand, which permits a closed form solution for the demand hazard to be obtained (e.g. [4-8]). This closed-form solution will provide a reasonable estimate of the demand hazard in the range of exceedance rate that the constants of Equation (1) are fitted. There are several methods of fitting these parameters, for example it was proposed [8] that the curve defined by Equation 1 be fitted through seismic hazard data at the Design Basis Earthquake (DBE) and Maximum Considered Earthquake (MCE) intensity levels which have 10% and 2% probabilities of exceedance in 50 years, respectively. Constraining the curve to pass through these points yields the following parameter values:

$$k = \frac{\ln\left(\frac{v_{DBE}}{v_{MCE}}\right)}{\ln\left(\frac{IM_{MCE}}{IM_{DBE}}\right)}, \quad k_0 = v_{DBE} (IM_{DBE})^k \quad (2)$$

where  $IM_{DBE}$ ,  $IM_{MCE}$ ,  $v_{DBE}$ ,  $v_{MCE}$  are the ground-motion intensities and annual rates of exceedance at the DBE and MCE intensity levels, respectively; and  $\ln(\cdot)$  is the natural logarithm of  $(\cdot)$ . A typical comparison of a seismic hazard curve for a Wellington (NZ) site (obtained by performing PSHA) and Equation (1) is given in Figure 1. It can be seen that due to the typical 'concave from below' shape of the hazard curve, Equation (1) significantly over estimates the hazard for ground-motion intensities below the DBE and above the MCE intensity levels, respectively. Equation (1) also slightly underestimates the hazard for intensities between the DBE and MCE levels. For example, at  $IM = 0.1g$  Sa, Equation (1) over predicts the rate of exceedance by a factor of eight. Hence, while the power law is an adequate local approximation to the hazard curve in the vicinity of the DBE and MCE, over several orders of magnitude the rate of exceedance,  $v$ , is poorly approximated (i.e. from  $v = 10^0$ - $10^{-6}$ ).

This inadequacy of Equation (1) is not significant for performance-based design if only a small range of exceedance frequencies are considered (and hence Equation (1) can be fitted

appropriately for this range). However, for financial risk calculations, where the full range of the hazard is of interest the use of the power law model will lead to significant inaccuracies. Previous researchers [9] have tried to alleviate this inaccuracy for more frequent earthquake events by only considering rates of exceedance up to a certain threshold value when using the power law model. The value of this threshold is however subjective and consequently not applicable in general. Others [10] have tried fitting a lognormal distribution to the data, but its implementation is difficult as it cannot consider rates greater than one and its parametric form involves the error function,  $\text{erf}(\cdot)$ .

While it is possible to perform PBEE calculations using the raw data from the seismic hazard curve directly, for certain sites the hazard data provided is sparse and significant interpolation between the data points is required; e.g. Kunnath *et al.* [11] used Equation 1 to interpolate between three hazard data points.

Therefore, it can be seen that a parametric curve which is non-linear in log-log space and more accurately captures the actual hazard data is required for use in financial risk assessments. This paper aims at developing improved parametric seismic hazard curves based on the above objectives. A semi-analytical closed form solution for the demand hazard using the new hazard model is presented, allowing the demand hazard to be computed without requiring numerical integration. This allows the use of the proposed hazard model in 'rapid' calculations of the demand hazard, similar to the analytical solution that can be obtained utilizing Equation (1), but with significantly enhanced accuracy over a large range of demand.

## **HYPERBOLIC MODEL IN LOG-LOG SPACE**

### **Model Development**

As the shape of the hazard curves typically have a 'concave from below' global shape (in log-log space), then it would seem reasonable to approximate the curve with a hyperbola of

the form  $y=\alpha/x$ . Figure 2 illustrates the use of a reference origin that can be used to envisage how the hyperbola can be expressed in the  $\ln(v)-\ln(IM)$  plane. The parametric curve has both vertical and horizontal asymptotes and is given by:

$$\ln(v) - \ln(v_{asy}) = \frac{\alpha}{\ln(IM) - \ln(IM_{asy})} + \varepsilon \quad (3)$$

where  $v_{asy}$  and  $IM_{asy}$  are the horizontal and vertical asymptotes, respectively;  $\alpha$  is constant; and  $\varepsilon =$  a random variable representing uncertainty with mean zero and standard deviation  $\beta_H$ . Hence by rearranging, Equation (3) can be expressed as either a function of  $v$  or  $IM$ , the median values of which are given in Equation (4). The three unknown parameters  $v_{asy}$ ,  $IM_{asy}$ , and  $\alpha$  are determined using data fitting techniques, as described in the following sub-section.

$$\hat{v} = v_{asy} \exp \left[ \alpha \left\{ \ln \left( \frac{IM}{IM_{asy}} \right) \right\}^{-1} \right] \quad (4a)$$

$$I\tilde{M} = IM_{asy} \exp \left[ \alpha \left\{ \ln \left( \frac{v}{v_{asy}} \right) \right\}^{-1} \right] \quad (4b)$$

The random variable,  $\varepsilon$  (Equation (3)), can be used to account for epistemic (modelling) uncertainty in the seismic hazard. This epistemic uncertainty is obtained through the use of logic tree weightings for different ground-motion prediction relationships [12-14].

### **Fitting to PSHA data**

To determine the parameters of the proposed hazard equation for given hazard data, the technique of (non-linear) least-squares regression was used. In the following discussions the hyperbolic model is used in the form of Equation (4a), so that errors are measured as deviations of  $v$  between the data and the model. As the overall shape of the hazard curve is of interest then it is desired to minimise the relative error between the data and the proposed curve and not the absolute error. The latter would lead to very accurate prediction of the data with large values of  $v$ , but poor prediction of small values. Equivalently, it is typical to minimise the logarithms of the error; then the least squares problem becomes:

$$\text{Minimise } R = \sum_{i=1}^n r_i^2 = \sum_{i=1}^n [\ln(v_i) - \ln(v(IM_i))]^2 \quad (5)$$

where  $v_i$  = data points obtained via PSHA;  $v(IM_i)$  = value of  $v$  obtained from parametric equation; and  $r_i$  = the least square residual for each data point.

A measure of the ‘goodness-of-fit’ of the parametric curve to the seismic hazard data can be objectively determined from the standard deviation (denoted as  $\beta_F$ ) of the residuals,  $r_i$ , obtained from the regression analysis. The lower the value of  $\beta_F$ , the better the hyperbolic model fits the raw hazard data. Table 1 (discussed in the following section) gives the values of  $\beta_F$  for several regions in New Zealand.

## APPLICATION TO SEISMICITY DATA

To illustrate the applicability of the proposed hyperbolic model, seismic hazard curve data for the main centres in New Zealand was obtained from Stirling *et al.* [15]. When the least squares regression is performed for both Peak Ground Acceleration (PGA) and elastic Spectral Acceleration ( $S_a$ ) at a period of 1.5 seconds then Figures 3a and 3b result. It can be seen that the accuracy of the hyperbolic model is maintained over the full range of data for both regions of high and low seismicity. Only the PGA seismic hazard curve for Dunedin is poorly approximated by the parametric curve due to its large ‘curvature’ for large IM values and then smaller curvature at lower IM values (here curvature refers to the second derivative of the curve in log-log space). In this case, it was selected to perform the regression on the data corresponding to the higher values of IM. This was selected because larger IM values will likely cause more structural damage and therefore have more engineering significance. Hence, for the Dunedin hazard data the first three data points were removed from the least-squares regression. The values of the three parameters for each of the PGA seismic hazard curves in Figure 3 and the associated standard deviations from the regression analyses are presented in Table 1.

As with any curve fitting of data, the primary limitation of the parametric curve given by Equation 4 is its use in extrapolation. Asymptotes on the maximum rate of exceedance and ground-motion intensity are requirements based on physical principles. The parametric relationship proposed has both horizontal and vertical asymptotes. However, because the parameters of the relationship are determined based on the data points within a specific range, the values of the asymptotes may not be consistent with those of different regions. Overall the range of hazard up to return periods of one million years ( $\nu = 1 \times 10^{-6}$ ) would be considered as sufficient to use for the assessment (in particular, calculating EAL which requires integration over the full range of IM), and therefore in the opinion of the authors no extrapolation of the parametric curve is required to obtain suitably accurate results when conducting performance-based assessments.

## **APPLICATION TO PROBABILISTIC SEISMIC DEMAND ANALYSIS**

In the following two sections the propagation of the effects of the seismic hazard curve is investigated through probabilistic seismic demand analysis (PSDA) by computing the drift hazard curve for a typical bridge pier designed to New Zealand standards [16].

### **Bridge details**

The prototype bridge pier is 7m high and taken from a typical ‘long’ multi-span highway bridge on firm soil with 40m longitudinal spans and a 10m transverse width. The seismic weight of the superstructure was calculated to be 7000 kN. The bridge was assumed to be located in Wellington, New Zealand, The fundamental period of the pier was 0.6 seconds. A computational model of the bridge pier was constructed using the nonlinear finite element program Ruaumoko [17]. The pier was modeled as a Single-Degree of Freedom (SDF), with a modified Takeda hysteresis model [18] for the force-displacement response of the pier column, and 5% viscous damping was assumed. The computation model was

calibrated based on experimental results [19].

Further design details and experimental modelling of the pier can be found elsewhere [19,20].

### **Site seismic hazard**

Seismic hazard data for the site was obtained from Stirling *et al.* [15]. The IM selected was the elastic spectral acceleration at the fundamental period of the structure, as it typically gives rise to a low dispersion ('efficiency') in the structural demand-response (IM-EDP) relationship, and is generally independent of magnitude and source-distance for carefully selected ground-motion records ('sufficiency') [7,21,22]. From the hazard data, both power law (Equation (1)) and hyperbolic (Equation (4)) parametric equations were fitted to the data, as shown in Figure 4a.

### **Structural response analysis**

Due to the lack of large earthquakes in the Wellington region over the past 100 years, despite its known high seismicity, there are insufficient regional ground-motion records to carry out a performance-based assessment. Therefore a suite of ground-motion records, previously used by Vamvatsikos and Cornell [23] were adopted, and are presented in Table 2. These records, which were all recorded on firm soil, have magnitude and distance ranges of 6.5-6.9 and 15.1-31.7 km, respectively.

Using the computational model of the bridge pier, Incremental Dynamic Analysis (IDA) [24] was conducted to generate the data to characterise the conditional IM-EDP relationship. The IDA was carried out using the elastic spectral acceleration at the fundamental period of vibration as the intensity measure (IM), and the maximum deck drift as the engineering demand parameter (EDP). The resulting IDA data from the structural analyses is presented in Figure 4b. The conditional IM-EDP relationship was then parameterized using Equation (8) developed by Shome and Cornell [25], which is based on separating the mutually exclusive

and collectively exhaustive cases of structural collapse and non-collapse, and a power law expression to describe the IM-EDP relation given collapse does not occur.

$$P(EDP > edp|IM) = P(EDP > edp|IM, NC)[1 - P(C|IM)] + P(C|IM) \quad (8)$$

where  $P(C)$  = the probability of collapse; and  $P(EDP > edp|IM, NC)$  is calculated by assuming EDP given IM ( $EDP|IM$ ) is lognormally distributed with logarithmic mean given by Equation (9), and lognormal standard deviation (dispersion)  $\beta_{\ln EDP|IM}$ .

$$\mu_{\ln EDP|IM} = \ln(a) + b \cdot \ln(IM) \quad (9)$$

where  $a$  and  $b$  are empirical constants determined by regression on the IDA data.

The 16<sup>th</sup>, 50<sup>th</sup> and 84<sup>th</sup> percentile curves (16<sup>th</sup> and 84<sup>th</sup> percentiles are one standard deviation from the median) are shown on Figure 4b. The bridge was deemed to collapse at a drift of 4% due to significant P- $\Delta$  effects from the superstructure. The aleatoric uncertainty,  $\beta_{\ln EDP|IM}$ , in the EDP for a given IM was modeled using a hyperbolic tangent function, while the variation of the collapse probability with IM was assumed to follow a lognormal distribution [21]. A comparison of the parametric fits for dispersion and collapse probability and the raw data points are presented elsewhere [26].

### Displacement hazard

Using both the seismic hazard and IDA parametric curves the displacement hazard of the pier can be obtained using the convolution integral presented by Deierlein *et al.* [27]:

$$\nu(EDP > edp) = \int P(EDP > edp | IM) |d\nu(IM)| \quad (10)$$

where the integration is over a range of IM values which have significant influence on the solution.

Equation (10) is then computed using numerical integration, the results of which are presented in Figure 5. It can be seen that in the immediate region surrounding the DBE and MCE levels the drift hazard curves given by the hyperbolic model and the power law model are similar. This is as to be expected considering the power law curve is fitted through the

DBE and MCE data points. However, as expected the power law relationship significantly over-predicts the drift hazard in the region of  $v > v(\text{DBE})$ . While the power law relationship also over-predicts the EDP for more intense ground-motions ( $v < 5 \times 10^{-4}$ ), it is not as significant as would be expected based on the shape of the seismic hazard curves. The reason for this can be attributed to the fact that for these more intense ground-motions, the EDP exceeds the drift representing structural collapse, which is illustrated by the ‘flattening’ of the drift hazard curves around  $v \sim 2 \times 10^{-4}$ . Therefore, it can be said that the extent of over-prediction of the power law relationship in the region of large ground-motion intensities is dependent on the seismic capacity of the structure.

## **A SEMI-ANALYTICAL CLOSED-FORM SOLUTION FOR ANNUAL FREQUENCY OF DEMAND**

The attractiveness of the power law model is that it can be used to obtain a closed form solution for the frequency of exceedance of demand (herein referred to as drift hazard) for a given structure at the site of interest. The mathematical form of the hyperbolic model does not directly permit such a solution. However, by inspection and appropriate modification of the closed form solution utilizing the power law hazard model, it is possible to obtain a semi-analytical solution for the drift hazard using the proposed hyperbolic model. Details of this semi-analytical solution are presented in this section. Note that unlike Figure 5 in the previous section (which uses Equations (8)-(10)), the closed form solution discussed in this section does not consider the onset of structural collapse. The potential incorporation of structural collapse is addressed in the discussion.

### **Mathematical details**

It has been shown [4-8] that by using power law relationships for the median seismic hazard (Equation (1)) and structural response (Equation (9)) relationships, and assuming the

IM-EDP relationship is lognormally distributed with constant dispersion ( $\beta_{EDP|IM}$ ), a closed form solution for the demand hazard can be obtained, as given by Equation (11):

$$v(EDP > edp) = k_0 \left( \frac{edp}{a} \right)^{-\frac{k}{b}} \exp \left( \frac{1}{2} \frac{k^2}{b^2} \beta_{EDP|IM}^2 \right) \quad (11)$$

where  $\exp(\bullet)$  is the exponential function. Jalayer [8] then suggested simplifying the presentation of Equation (11) by introducing the idea of the “*im* that corresponds to *edp*” defined as:

$$IM^{edp} = \left( \frac{edp}{a} \right)^{\frac{1}{b}} \quad (12)$$

Equation (12) is also the solution of Equation (9) for a given *edp* value. This can be interpreted as the IM value corresponding to the EDP, from the median IM-EDP relationship. This then allows Equation (11) to be expressed as follows:

$$v(EDP > edp) = k_0 (IM^{edp})^{-k} \exp \left( \frac{1}{2} \frac{k^2}{b^2} \beta_{EDP|IM}^2 \right) = v(IM^{edp}) \exp \left( \frac{1}{2} \frac{k^2}{b^2} \beta_{EDP|IM}^2 \right) \quad (13)$$

Hence, from the right hand side of Equation (13), the demand hazard can be viewed as the value obtained from the median seismic hazard (Equation (1)) and median demand (Equation (9)) relations and an exponential term, which represents the increase in the hazard due to uncertainty. In particular the exponential term is a function of *k*.

Firstly, the ‘median demand hazard’ (defined as  $v(IM^{edp})$  in Equation 13) for a given EDP value, can be determined by using the hyperbolic model by computing  $IM^{edp}$  from Equation (12) and then using Equation 4a with  $IM = IM^{edp}$ .

Secondly, it should be noted that geometrically *k* is simply a local approximation of the gradient of the seismic hazard curve in log-log space. The only difference between the power law and hyperbolic hazard models in this regard is that *k* is constant for the power law model, but not for the hyperbolic model. Hence, by differentiating Equation (3) with respect to  $\ln(IM)$ , the equivalent local gradient of the hyperbolic model is given by:

$$k_{eq} = \frac{\partial[\ln(v(IM))]}{\partial[\ln(IM)]} = \frac{-\alpha}{\left[\ln\left(\frac{IM}{IM_{asy}}\right)\right]^2} \quad (14)$$

where  $k_{eq}$  = equivalent local gradient of the seismic hazard curve in log-log space, and the value of IM to be used is discussed below.

It would seem intuitive that the IM value to be used (in Equation 14) would be  $IM^{edp}$ . Figure 6 presents the values of the drift hazard curve obtained using  $IM = IM^{edp}$  to compute  $k_{eq}$  in Equation (14), compared to the computed ‘median demand hazard’ ( $v(IM^{edp})$ ), and the ‘exact demand hazard’ (which is obtained by direct numerical integration of Equation (10)). It is immediately obvious that the exponential term (the factor in Equation 13 giving rise to the difference between the median demand hazard curve and the exact demand hazard) is too large. This occurs because for a given value of EDP, the median ground-motion hazard value is always smaller than the exact ground motion hazard value. From Figure 3 it can be seen that the slope of the hyperbolic hazard curve increases (in absolute terms) as  $v(IM > im)$  decreases. Therefore using  $IM = IM^{edp}$  gives an unreasonably large  $k_{eq}$ , which is further amplified within the exponential term. Use of the mean (as opposed to median) demand curve does not resolve this problem. Therefore  $k_{eq}$  should be obtained using Equation 4b as before, but should be the IM corresponding to the ‘exact demand hazard’ value, as opposed to the ‘median demand hazard’ value. As the ‘exact demand hazard’ value is not actually known, implementing the equation in this form requires an iterative process.

This problem of what slope,  $k_{eq}$  (or  $k$ ), to use to compute  $v(EDP)$  is not just a problem with using the hyperbolic model (Equation (4)), but is also a problem when using the closed-form solution for the power law model (Equation (13)). This problem can be resolved if the closed form solution is inverted, therefore becoming a function of  $v$ . Hence, the solution procedure is as follows: (i) for the selected rate of exceedance calculate the log-log slope,  $k_{eq}$ , of the hazard curve; and (ii) calculate the EDP using the selected rate of exceedance and  $k_{eq}$ .

Since both the approximation for the slope and the corresponding EDP are calculated based on the same rate of exceedance, then the solution should be more accurate, without requiring iteration.

Inverting the closed form solution proposed by Luco and Cornell [2] (Equation (11)) gives the EDP for a given rate of exceedance,  $\nu$ :

$$EDP(\nu) = a \left( \frac{\nu}{k_0} \right)^{-\frac{b}{k}} \exp \left( \frac{1}{2} \frac{k}{b} \beta_{EDP|IM}^2 \right) \quad (15)$$

Calculation of  $EDP(\nu)$  using the hyperbolic hazard model can be determined by starting with Equation (13), where  $\nu(IM^{edp})$  is given by substituting Equation (12) into Equation (4a). Then the log-log slope of the hazard curve,  $k$ , can be expressed as a function of  $\nu$  by substituting Equation (4b) into Equation (14). Finally, this modified form of Equation (13) can be rearranged as a function of EDP to yield:

$$EDP(\nu) = aIM_{asy}^b \exp \left[ \frac{ab}{V - \frac{V^4}{2b^2\alpha^2} \beta_{EDP|IM}^2} \right] \quad (16)$$

where  $V = \ln(\nu/\nu_{asy})$ , and all other parameters have their usual meaning.

Figure 7 illustrates the approximation of Equation (16) to the ‘exact’ solution obtained via numerical integration, compared with the closed form solution using the power law hazard model (Equation (15)). It can be seen that the semi-analytical closed form solution displays far superior accuracy over a larger range of EDP, in comparison to the power law closed form solution. The semi-analytical solution is not exactly the same as the numerical solution however. The reason for this is that the convolution integral (e.g. Equation (10)) is dependent on the hazard at various intensity levels (i.e. the integration is over the full range of IM) and therefore at these different intensity levels the value of  $k$  varies. The semi-analytical solution, however, uses only a constant  $k$  value corresponding to the rate considered. For the bridge

pier case study drift hazard curves (Figure 7) this over prediction ranged from 5-10% with a mean value of 7%. Even despite this inconsistency, the accuracy is sufficient considering the simplification of a closed form solution over numerical integration.

## DISCUSSION

The previous sections have illustrated that probabilistic seismic demand analysis (PSDA) carried out analytically using the proposed hyperbolic model gives results which are significantly more accurate compared to those obtained using the closed form solution presented by others [4-8].

Note that the procedure to obtain the semi-analytical solution presented is not unique to the seismic hazard model used. For example, the authors investigated the use of more classical probability distributions to model the hazard, such as the lognormal cumulative distribution function (CDF), i.e:

$$\nu = 1 - \left[ \frac{1}{2} + \frac{1}{2} \operatorname{erf} \left( \frac{\ln IM - \mu}{\sqrt{2}\sigma} \right) \right] \quad (17)$$

where  $\operatorname{erf}$  = is the error function; and  $\mu$ ,  $\sigma$  are the logarithmic mean and standard deviation of the lognormal CDF. The same procedure can be used to obtain the solution for EDP( $\nu$ ). The final form of EDP( $\nu$ ) is significantly more complicated, and is given by:

$$EDP(\nu) = a \exp \left[ b\mu + \sqrt{2}b\sigma \operatorname{erf} \operatorname{inv} \left( 1 - 2\nu \exp \left\{ -\frac{1}{2} \frac{k^2}{b^2} \beta^2 \right\} \right) \right] \quad (18)$$

$$k = \frac{1}{\sigma\nu\sqrt{2\pi}} \exp \left( -\left\{ \operatorname{erf} \operatorname{inv} (1 - 2\nu) \right\}^2 \right)$$

where  $\operatorname{erf} \operatorname{inv}$  = the inverse error function. Also, the ability of the lognormal distribution in approximating the hazard curve is somewhat limited (in certain cases) compared to the proposed hyperbolic model, in that it only has two parameters (mean and standard deviation) compared to the three for the hyperbolic model, making its fit of the hazard data less flexible.

As it has been shown that the ‘curvature’ of the hazard model can now be incorporated into the closed form solution, the only limitation of Equation 16 (or Equation 18 for that matter), is that the demand model parametric equation (Equation 9) does not typically model the response in the region of global collapse well [3]. Shome and Cornell [21] showed that by using a power law function to describe the probability of collapse, a closed form solution could be obtained which considers collapse in the demand model. The (simple) inclusion of collapse using the proposed hyperbolic model (or lognormal model) could be the subject of further work.

## CONCLUSIONS

Based on the findings of this research the following conclusions can be drawn:

1. A novel hazard model has been developed which is non-linear in log-log space. The model is typically fitted to seismic hazard data via least squares regression, and it allows for the incorporation of epistemic uncertainty in the hazard.
2. The applicability of the model to seismic hazard data in New Zealand has been illustrated for both PGA and spectral acceleration and results for PGA have been tabulated.
3. Via a performance-based assessment of a bridge pier designed to New Zealand standards, it has been illustrated that the power law model for the seismic hazard significantly over-estimates the demand hazard if used over a wide range of EDP, and the proposed hyperbolic seismic hazard model has proved to be a much more reliable option.
4. A semi-analytical solution procedure to calculate the drift hazard in closed-form has been proposed. The procedure, while not exact, had an mean relative over-

prediction of 7% for the given example. The proposed procedure is therefore a viable alternative compared to the closed-form solution utilizing the power law hazard model.

## **ACKNOWLEDGEMENTS**

The authors would like to acknowledge Dr Graeme McVerry, from the Institute of Geological and Nuclear Sciences (GNS) for providing the PSHA data for New Zealand regions.

## REFERENCES:

1. Esteva L. Criteria for the construction of spectra for seismic design. *Third Panamerican Symposium on Structures* 1967, Caracas, Venezuela.
2. Esteva L. Bases para la formulación de decisiones de diseño sísmico. *Ph.D Dissertation* 1968. Universidad Nacional Autónoma de México, Mexico City
3. Cornell CA. Engineering seismic risk analysis. *Bulletin of the Seismological Society of America* 1968; **58**(5): 1583-1606
4. Sewell RT, Toro GR, McGuire RK. Impact of ground motion characterisation on conservatism and variability in seismic risk estimates. *NUREG/CR-6467. U.S. Nuclear Regulatory Commission*, Washington, DC. 1991
5. Kennedy RP, Short SA. Basis for Seismic Provisions of Doe-Std-1020. Ucll-Cr-111478 and Bnl-52418. *Lawrence Livermore National Laboratory and Brookhaven National Laboratory*. 1994
6. Cornell CA. Reliability-Based Earthquake-Resistant Design – the Future. *11<sup>th</sup> World Conference on Earthquake Engineering*. 1996
7. Shome N, and Cornell CA. Probabilistic seismic demand analysis of nonlinear structures. *Report No. RMS-35, RMS Program* 1999, Stanford University, Stanford, CA.
8. Jalayer F. Direct Probabilistic Seismic Analysis: Implementing Non-linear Dynamic Assessments. *Ph.D Dissertation* 2003. Department of Civil and Environmental Engineering, Stanford University. California. USA
9. Mander JB, Dhakal RP, Mashiko N, Solberg KM. Incremental dynamic analysis applied to seismic financial risk assessment of bridges. *Engineering Structures*. (In Press).
10. Lee TH, Mosalam K. Probabilistic Seismic Evaluation of Reinforced Concrete Structural Components and Systems, PEER report number 2006/04, Stanford University, California, USA. <http://peer.berkeley.edu>.
11. Kunnath SK, Larson L, Miranda E. Modelling Considerations in Probabilistic Performance-based Seismic Evaluation: Case Study of the I-880 Viaduct, *Earthquake Engineering and Structural Dynamics* 2006, **35**(1): 57-75.
12. Kramer SL. *Geotechnical earthquake engineering*. Prentice Hall: Upper Saddle River, N.J, 2006. 137-138
13. Kulkarni RB, Youngs RR, and Coppersmith KJ. Assessment of confidence intervals for results of seismic hazard analysis. *Proceedings of the Eighth World Conference on Earthquake Engineering* 1984, San Francisco, vol. 1, 263-270.
14. Bommer JJ, Scherbaum F, Bungum H, Cotton F, Sabetta F, and Abrahamson NA. On the use of logic trees for ground-motion prediction equations in seismic hazard assessment.

*Bulletin of the Seismological Society of America* 2005. **95**(2), 377-389.

15. Stirling MW, McVerry GH, Berryman KR. A New Seismic Hazard Model for New Zealand, *Bulletin of the Seismological Society of America* 2002. **92**(5): 1878-1903.
16. Standards New Zealand. NZS 3101: Part 1: 1995: *Concrete Structures Standard*, Standards New Zealand, Wellington.
17. Carr AJ. Ruaumoko: Inelastic Dynamic Computer Program. *Computer Program Library* 2004, Department of Civil Engineering, University of Canterbury, Christchurch, New Zealand.
18. Otani S. SAKE, A Computer Program for Inelastic Response of R/C Frames to Earthquakes. *Report UILU-Eng-74-2029* 1974, Civil Engineering Studies, Univ. of Illinois at Urbana-Champaign.
19. Dhakal RP, Mander JB, Mashiko N. Bidirectional Pseudodynamic Tests of Bridge Piers Designed to Different Standards. *Journal of Bridge Engineering ASCE* 2007. **12**(3): 284-295
20. Solberg KM. Experimental and analytical investigations into the application of damage avoidance design. *Master of Engineering Thesis* 2007. University of Canterbury, Christchurch, New Zealand.
21. Aslani H. Probabilistic Earthquake Loss Estimation and Loss Disaggregation in Buildings. *Ph.D. Thesis* 2005, John A. Blume Earthquake Engineering Centre, Dept. of Civil and Environmental Engineering, Stanford University, Stanford, CA: 382
22. Luco N, Cornell CA. Seismic drift demands for two SMRF structures with brittle connections. *Structural Engineering World Wide* 1998, Elsevier Science Ltd., Oxford, England, Paper T158-3.
23. Vamvatsikos D. Cornell CA. Applied Incremental Dynamic Analysis, *Earthquake Spectra* 2004, **20**(2): 523–553.
24. Vamvatsikos D. Cornell CA. Incremental Dynamic Analysis, *Earthquake Engineering and Structural Dynamics* 2002. **31**(3): 491–514.
25. Shome N, Cornell CA. Structural Seismic Demand Analysis: Consideration of “Collapse”. *8<sup>th</sup> ASCE Specialty Conference on Probabilistic Mechanics and Structural Reliability* 2000. University of Notre Dame, South Bend, Indiana.
26. Bradley BA, Dhakal RP, Mander JB. Parametric Structure Specific Seismic Loss Estimation, *4<sup>th</sup> International Conference on Urban Earthquake Engineering* 2007. Tokyo, Japan. Keynote lecture: 45-52.
27. Deierlein GG, Krawinkler H, Cornell CA. A Framework for Performance-based Earthquake Engineering. *Pacific Conference on Earthquake Engineering* 2003. Christchurch, New Zealand.

**Table 1: Hazard curve parameters for various regions to be used in Equation 4 for PGA**

<b>Region</b>	<b><math>v_{asy}</math></b>	<b><math>IM_{asy}</math></b>	<b><math>\alpha</math></b>	<b><math>\beta_F</math></b>
Auckland	98450	126	121.6	0.12
Wellington	6617	81.7	75.9	0.20
Christchurch	1221	29.8	62.2	0.06
Otira	9.95	10.5	20.5	0.14
Dunedin	1.8	10.3	26.3	0.13

**Table 2: Ground motion records used in seismic response analysis**

No	Event	Year	Station	$\phi^{*1}$	$M^{*2}$	$R^{*3}$ (km)	PGA (g)
1	Loma Prieta	1989	Agnews State Hospital	90	6.9	28.2	0.159
2	Imperial Valley	1979	Plaster City	135	6.5	31.7	0.057
3	Loma Prieta	1989	Hollister Diff. Array	255	6.9	25.8	0.279
4	Loma Prieta	1989	Anderson Dam	270	6.9	21.4	0.244
5	Loma Prieta	1989	Coyote Lake Dam	285	6.5	22.3	0.179
6	Imperial Valley	1979	Cucapah	85	6.9	23.6	0.309
7	Loma Prieta	1989	Sunnyvale Colton Ave	270	6.9	28.8	0.207
8	Imperial Valley	1979	El Centro Array #13	140	6.5	21.9	0.117
9	Imperial Valley	1979	Westmoreland Fire Sta.	90	6.5	15.1	0.074
10	Loma Prieta	1989	Hollister South & Pine	0	6.9	28.8	0.371
11	Loma Prieta	1989	Sunnyvale Colton Ave	360	6.9	28.8	0.209
12	Superstition Hills	1987	Wildlife Liquefaction Array	90	6.7	24.4	0.180
13	Imperial Valley	1979	Chihuahua	282	6.5	28.7	0.254
14	Imperial Valley	1979	El Centro Array #13	230	6.5	21.9	0.139
15	Imperial Valley	1979	Westmoreland Fire Sta.	180	6.5	15.1	0.110
16	Loma Prieta	1989	WAHO	0	6.9	16.9	0.370
17	Superstition Hills	1987	Wildlife Liquefaction Array	360	6.7	24.4	0.200
18	Imperial Valley	1979	Plaster City	45	6.5	31.7	0.042
19	Loma Prieta	1989	Hollister Diff. Array	165	6.9	25.8	0.269
20	Loma Prieta	1989	WAHO	90	6.9	16.9	0.638

<sup>1</sup> Component<sup>2</sup> Moment Magnitudes<sup>3</sup> Closest Distances to Fault RuptureSource: PEER Strong Motion Database, <http://peer.berkeley.edu/smcat/>

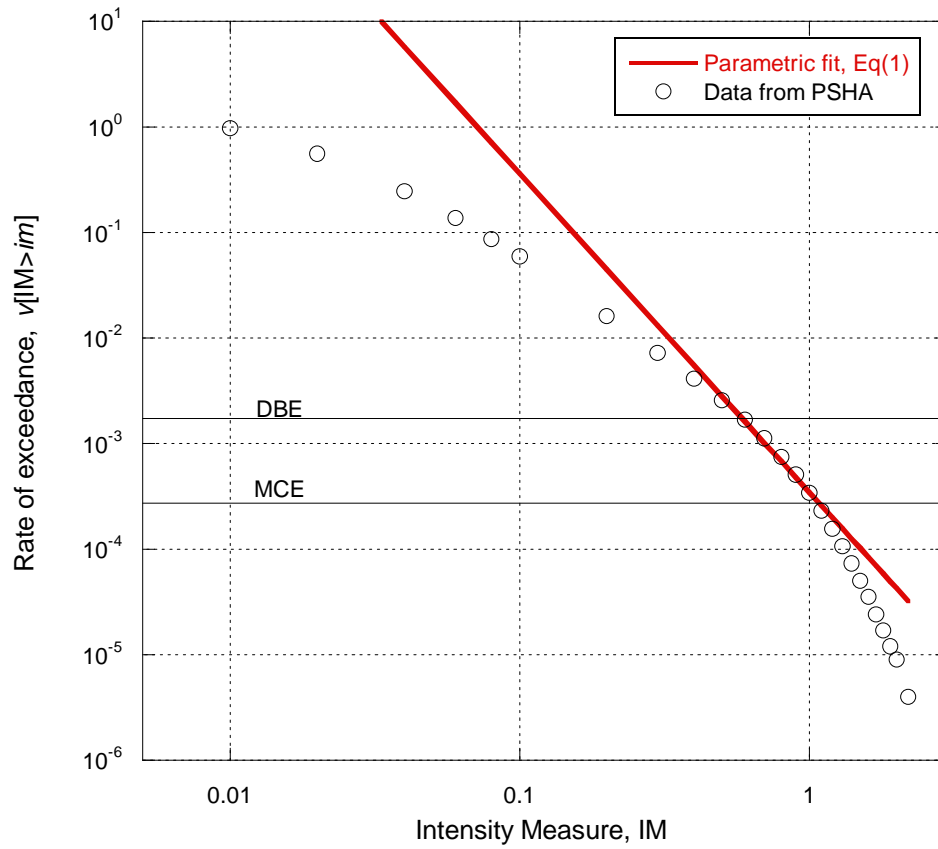


**Figure 1. Comparison on hazard data from PSHA fitted by Equation (1).**

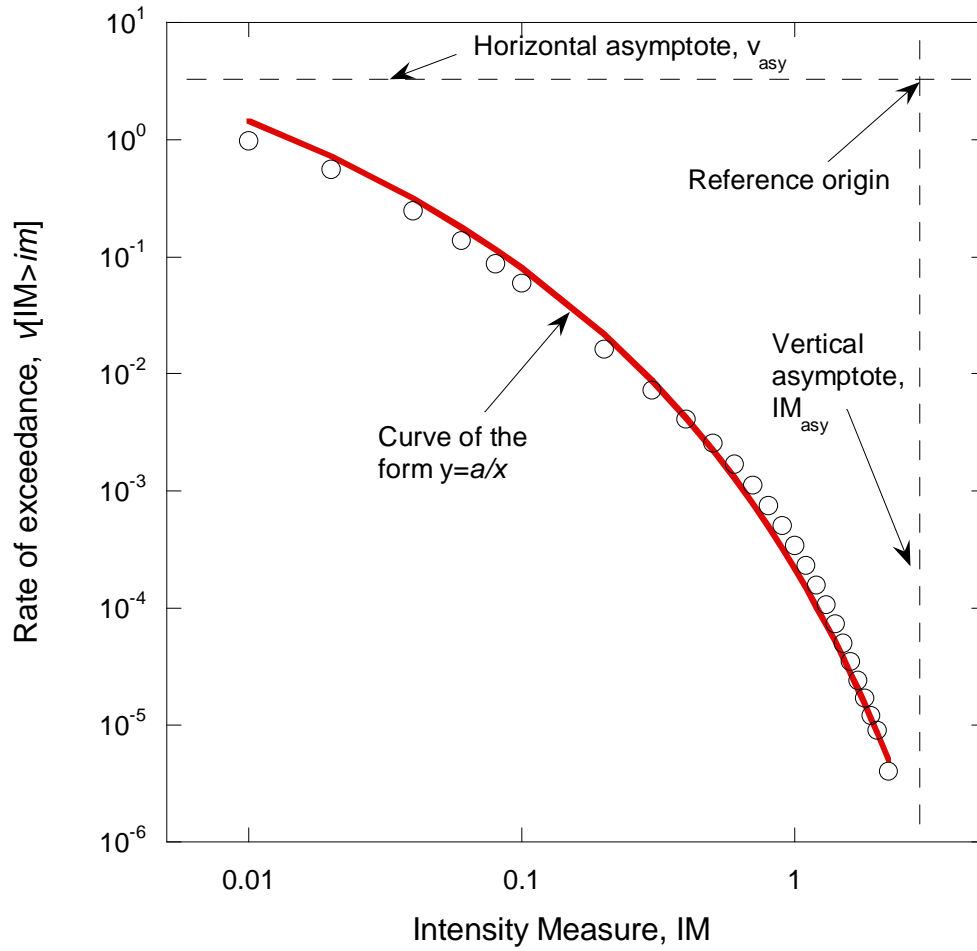


**Figure 2. Concept of hyperbolic curve fitted to hazard data.**

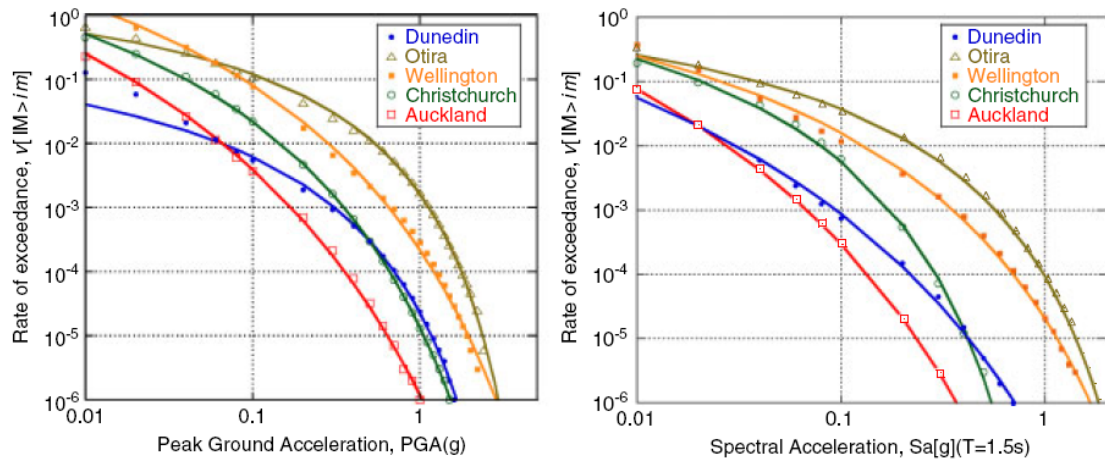


**Figure 3. Fitted seismic hazard PGA and Sa data for New Zealand: (a) seismic hazard data for PGA fitted using Equations (4a) and (4b) and (b) seismic hazard data for Sa( $T = 1.5$  s) fitted using Equations (4a) and (4b).**

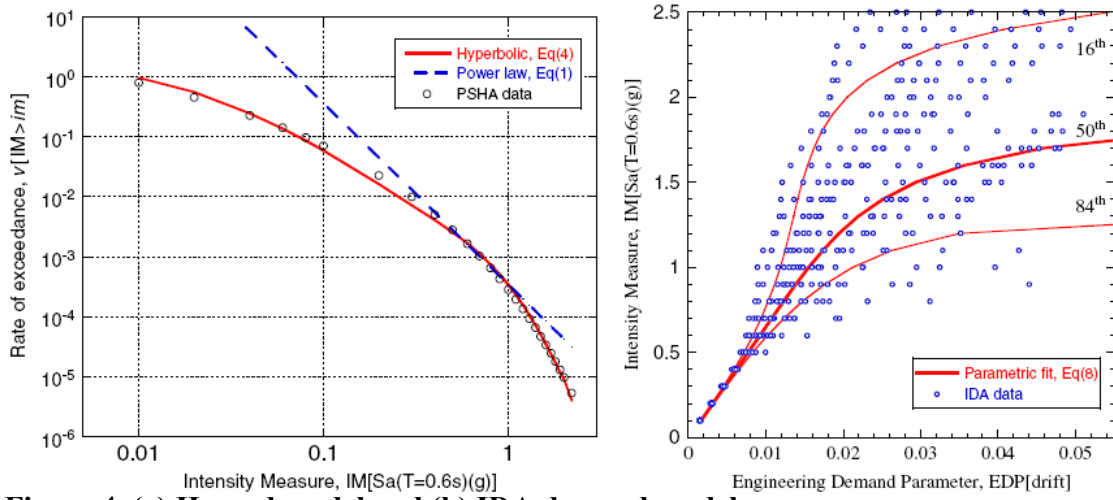


**Figure 4. (a) Hazard model and (b) IDA demand model curves.**

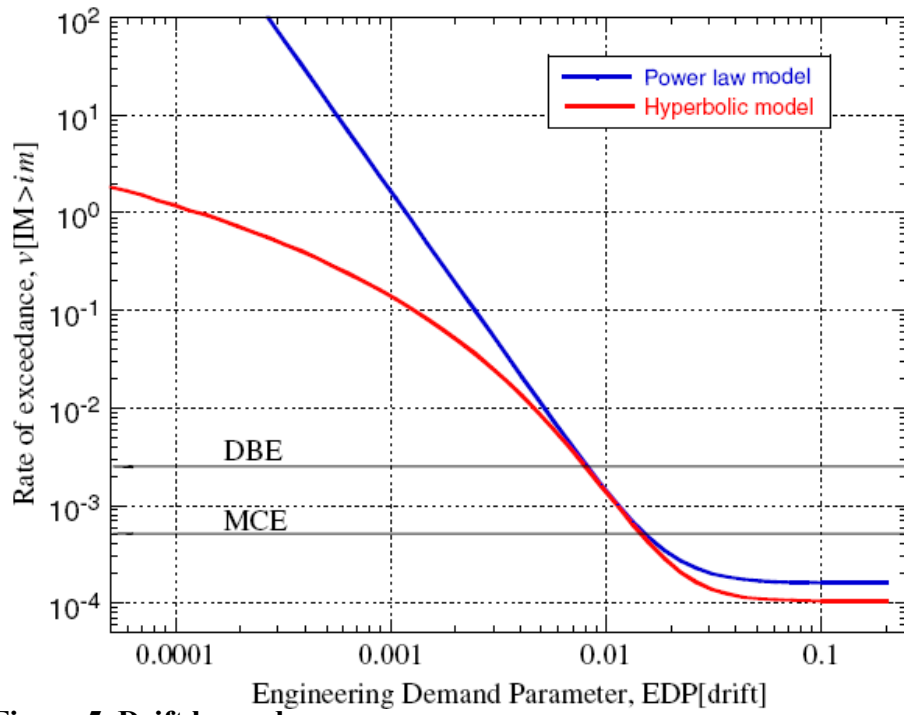
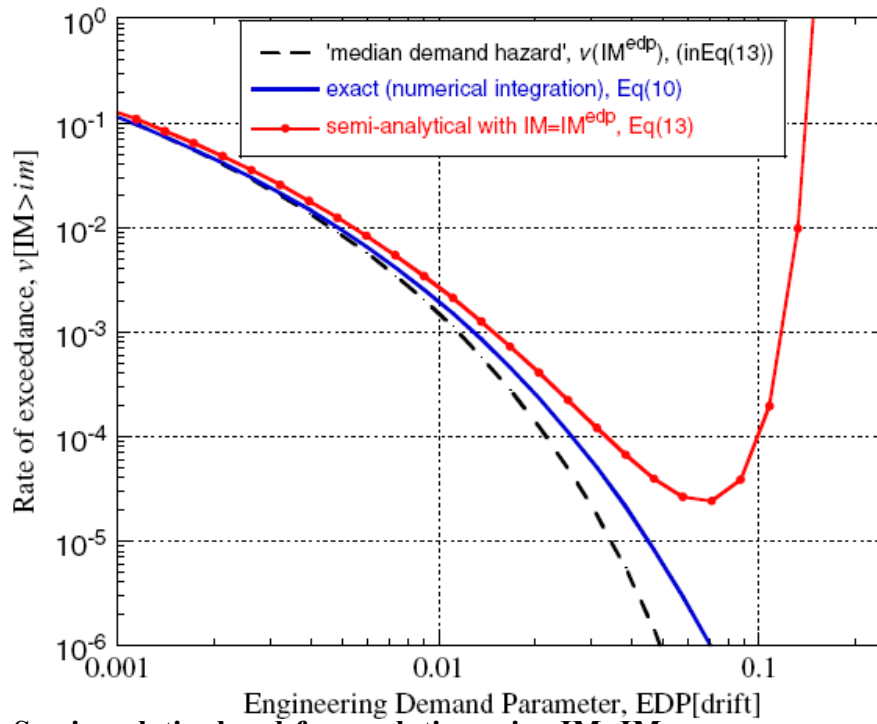
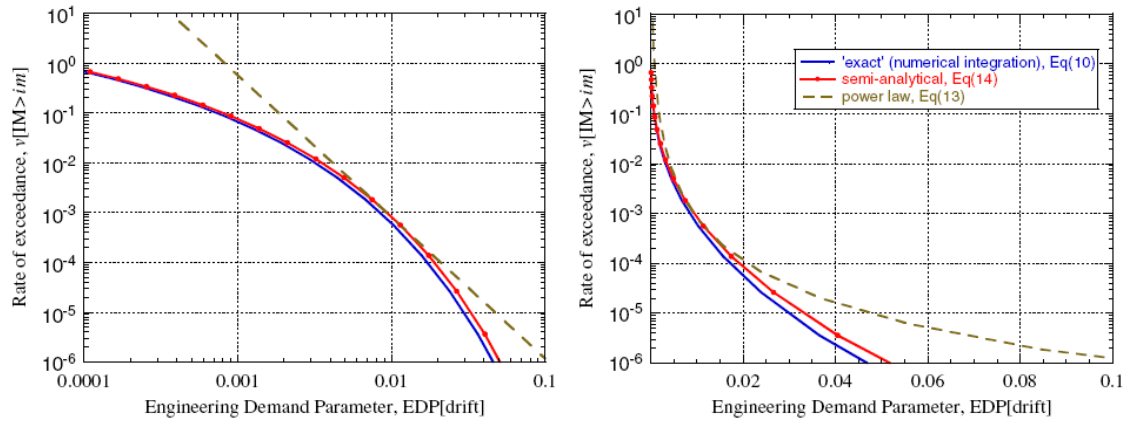


Figure 5. Drift hazard curves.



**Figure 6. Semi-analytic closed-form solution using  $IM=IM_{edp}$ .**



**Figure 7. Semi-analytic closed-form solution: (a) in  $\ln(IM)-\ln(v)$  space and (b) in  $IM-\ln(v)$  space.**